Journal of Physics: Conference Series

PAPER • **OPEN ACCESS**

Influence of leading edge shapes on vortex behaviour of delta wing

IOP Conf. Series: Journal of Physics: Conf. Series **1276** (2019) 012008 doi:10.1088/1742-6596/1276/1/012008

Influence of leading edge shapes on vortex behaviour of delta wing

M Ramakrishna[1], C Senthil Kumar[2] and B Venkatesh[1]

[1]Department of Aeronautical Engineering, Tagore Engineering College, Rathinamangalam, Chennai-600127, INDIA
[2] Department of Aerospace Engineering, Anna University, MIT Campus, Chennai-600045, INDIA

Abstract. This paper analyzes the vortex behaviour of three delta wing configurations namely plane delta wing, saw-tooth delta wing, and sinusoidal tooth delta wing. Experiments such as flow visualization at low speeds, oil flow visualization at different velocities are performed using a low speed wind tunnel. Experiments are conducted for different Reynolds number 0.25, 0.3 and 0.35 million at various angles of attack 10° to 40° in steps of 10°. CFD studies are also carried out by using commercially available software ANSYS FLUENT to have an insight of unsteady nature of vortices. Oil flow visualization study depicts two symmetric separation lines indicating symmetric vortices for all three delta wings at 10° and 20° angles of attack. It was also noticed that at 30° angle of attack plane delta shows asymmetric separation lines indicating asymmetric nature of vortices. Again at 40° angle of attack random pattern of oil traces are evident of flow separation and wake formation on the top surface of the wing. Plane delta has more area of random pattern compared to sinusoidal-tooth and saw-tooth delta wing. Results were authenticated with computational study and it is found that vortices are highly stable at 10° and 20° angles of attack for all planforms. At the same time vortices are found to be flip-flopping if angle of attack is increased to 30°, which in turns are governed by unsteady forces due to uneven pressure distribution.

1. Introduction

Delta wing is essentially a triangular planform to incorporate increase in lift coefficient without affecting the drag coefficient. The main advantage of delta wing over other wing planforms is that they delay stall thereby making the lift coefficient to increase steadily even at higher angles of attack. Delta wings demonstrate good aerodynamic characteristics at higher angles of attack compared to lower angles of attack. Owing to large root chord, a delta wing in combination less wing thickness and sufficiently thick wing spar provides light structure and high internal volume for fuel. Delta wings are preferred for supersonic aircrafts since they keep the wave drag within control. Also one of the main characteristics of a delta wing is the vortex lift. With sufficient leading edge sweep, a delta wing generates vortex lift so flow separation can be used as lift producing tool at the same time tends to delay the critical Mach number and drag divergence Mach number.

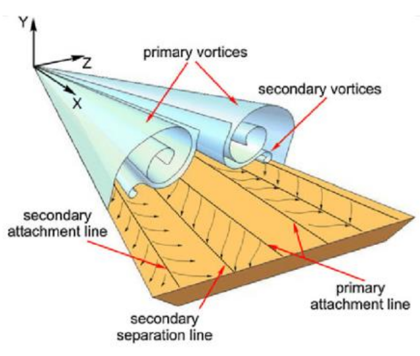

Figure 1. Schematic diagram of flow topology over a delta wing

2. Delta wing design

The current study involves the flow behaviour of delta wings having three different leading edge profiles as shown in figure 2. The design modifications are employed with an intention to make the vortices stable and steady with increase in angles of attack.

The basic configurations of all three delta wings are identical and fabricated using Aluminium metal.. Wings have root chord of 246.6mm, base of 230mm and sweep angle of 65°. All the tested wings contain thickness of 15mm with 45° chamfered edges. Also maximum thickness to chord ratio is retained as 6.09%. The wavelengths of both sinusoidal and saw tooth delta wings are 36mm.

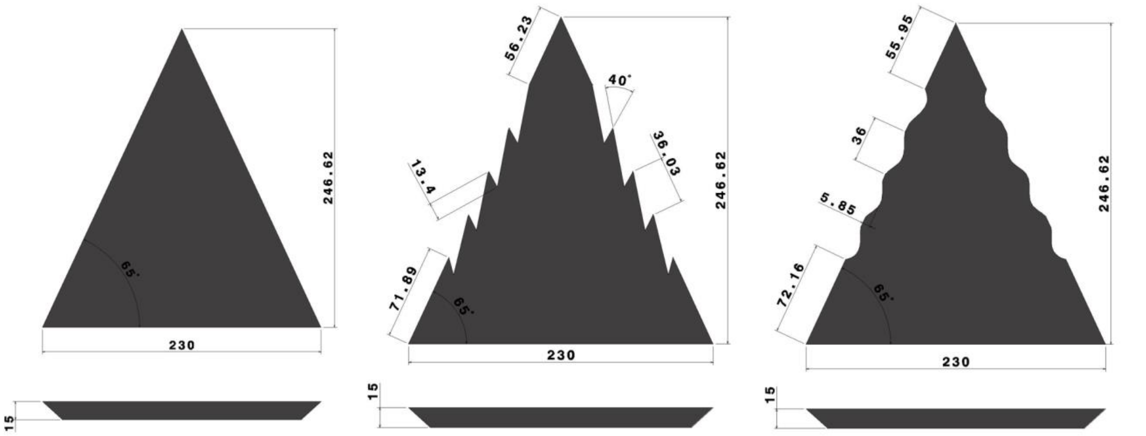

Figure 2. Dimensions of (a) Plane delta wing (b) Saw-tooth delta wing (c) Sinusoidal delta wing

3. Experimental setup and methodology

3.1. Test facility

The experiments have been carried out in a open circuit, subsonic wind tunnel of test section cross section 600mm x 600mm, length being 2 metres. The wind tunnel has four constant pitch propeller blades which is driven by a 20HP, 3 phase induction motor. The optimum speed of motor is 1500 rpm which corresponds to a velocity of 30m/s (By Calibration). A sector typed model mounting mechanism is utilized for mounting the model. This mechanism can pitch, and yaw from -10^0 to $+30^0$ and -20^0 to $+20^0$ respectively. For further increment in pitch angle an adapter made of mild steel is used. The wind tunnel was calibrated before the start of the experiments using a hot-wire anemometer and was found that turbulent intensity of 2%. For maximum angle of attack blockage ratio was observed to be about 5%.

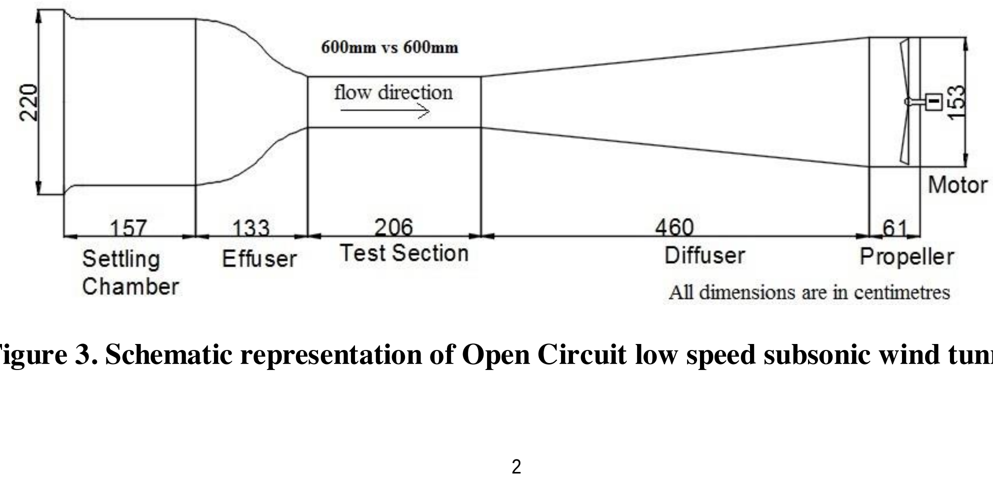

Figure 3. Schematic representation of Open Circuit low speed subsonic wind tunnel.

3.2. Laser smoke flow visualization

For insight of vortex behaviour over delta wings Laser-smoke flow visualization has been employed for angles 10^0, 20^0, 30^0 and 40^0 at 200 rpm corresponding to a test section velocity 3m/s. Fog machine rating 1200 W fog machine was used to initiate smoke. The fog machine was placed near to the inlet of the tunnel. A 100mW green laser pointer along with a Fresnel lens which translates the laser pointer to a line laser was mounted top of tunnel. To illuminate the smoke particles emitting from the nozzle of the fog machine as represented in figure 4.

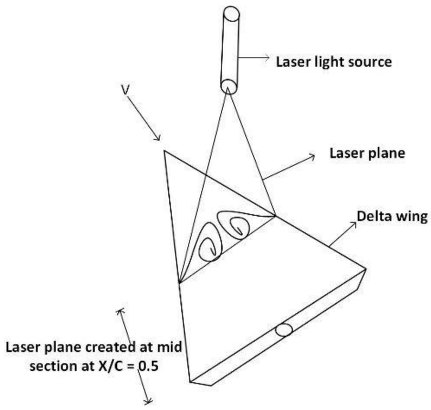

Figure 4. Principle of laser-smoke flow visualization

A laser plane is created on the mid plane of the delta wing perpendicular to the chord using the laser pointer and a Fresnel lens. High speed camera was employed to capture flow visualization.

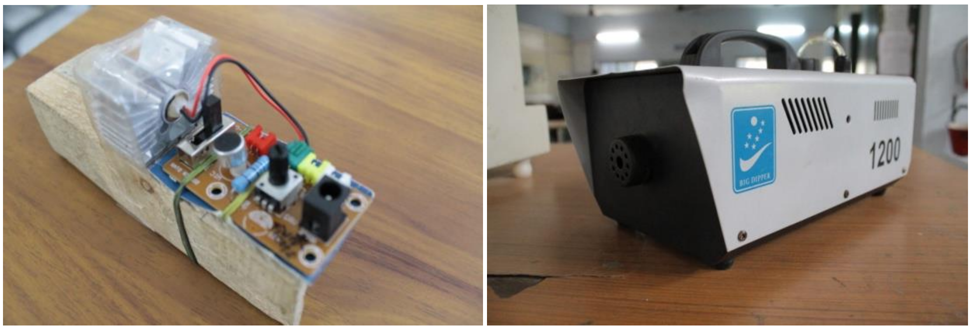

(a) **(b)**

Figure 5. (a) 100mW green laser (b) 1200W fog machine used for laser-smoke flow visualization

3.3. Oil flow visualization

Oil flow visualization technique is purely a two dimensional surface flow visualization technique that presents flow behaviour over a model surface. In turn the flow pattern over a model furnishes qualitative information of vortices. The oil contains mixture of nano graphite powder, oleic acid and few tiny drops of kerosene. Since nano graphite powder is white in colour therefore top surface of the model is painted black to enhance flow visibility. Oleic acid is used to increase the viscosity of the mixture. To ensure unaffected flow of oil wing surface finish was made smooth. The mixture should neither be too lean for free flow nor too thick to align with flow direction. The proportion of mixture depends on the atmospheric conditions and the surface finish of the model. Precautions must be taken that the delta wing must be kept in test section before the oil is spayed.

This visualization is done for angles of attack 10°, 20°, 30°and 40° at three different Reynolds numbers 0.25million, 0.3million and 0.35million for which the corresponding velocities are 15.37m/s, 18.44m/s and 21.51m/s. The Reynolds numbers are with respect to the root chord of the delta wing.

3.4. Computation methodology

Since oil flow and smoke flow visualization gives only an understanding of the flow behaviour over a delta wing, it is necessary to employ computation methodology and obtain quantitative results.. In this study, ANSYS FLUENT has been used as a tool for CFD analysis. A structured grid was employed for all the three wings with a rectangular domain. One grid was developed for each wing with 0.8million cell count. The orthogonal quality was checked for the grids before starting the analysis and it was found to be differing between 0.9 and 0.95 for three grids (maximum orthogonal quality is 1). The grids were made very fine for delta wing surface and some region around the wing in order to obtain better information.

The domain is made such that there a large area behind the model which will help us to study the wake formation due to the vortices of the delta wing. The direction along the flow (chordwise) is taken as X direction, spanwise direction is taken as Z direction and the direction perpendicular to the wing planform is Y direction. Hence the drag is considered along +X direction and lift is considered along +Y direction.

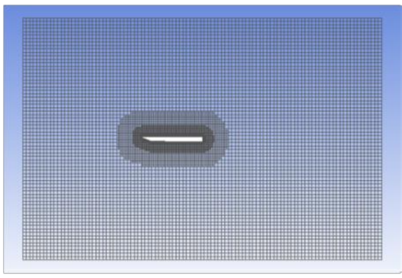

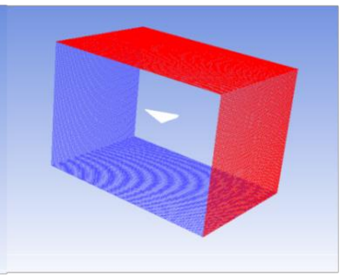

(a) **(b)**

Figure 6. (a) Cross section view of the grid in longitudinal plane (b) Delta wing inside the domain

The computation is performed for angles of attack 10°, 20°, 30°,and 40° at Reynolds number 0.25million, 0.3million and 0.35million (based on root chord). One grid is used for all the cases of each wing. The front and bottom surfaces of the domain are considered as inlet and the top and back surfaces are considered as outlet.

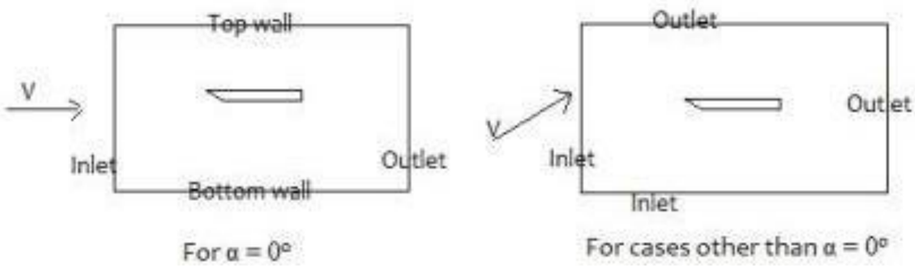

Figure 7. A view of grid boundary conditions.

Since vortices are unsteady flow phenomena, pressure based laminar unsteady incompressible second order solver with Least Square Method having SIMPLEC as pressure-velocity coupling has been chosen after a basic study on vortex capture methodology using ANSYS Fluent software.

Since unsteady computation is done, the time step size was taken as 0.01seconds and the total time steps were taken as 1000. The number of iterations was taken as 40 for each time step and therefore a total of 40,000 iterations were done for each of the 45 cases. Planes were created spanwise at mid chord and base to monitor the pressure contours which will give a better understanding of the generated vortices.

4. Discussion of results

4.1. Laser smoke flow visualization

Laser-smoke flow visualization performed gives us an insight of the vortices behaviour with for all increase in angles of attack for different leading edge profiles.

It is clearly evident that stable symmetric vortex patterns for all three delta wings at 10° angle of attack. As the angle of attack is increased to 20°, vortices become unstable and flip-flops at low frequency. At 30° it was observe a similar pattern as in case of 20^{0} but the flip flopping of vortices seems to be at higher frequency. Also at 20^{0} and 30^{0} the vortices were found to be lifted slightly from the top surface of the wing. At 40^{0} angle of attack, the flow becomes fully turbulent and visualization is vague. Also is clear from figure 8 that the vortices shed from the delta wing surface at 30^{0} and 40^{0} and at 40^{0}, both saw-tooth and sinusoidal delta wing generates a strong vortex at their teeth.

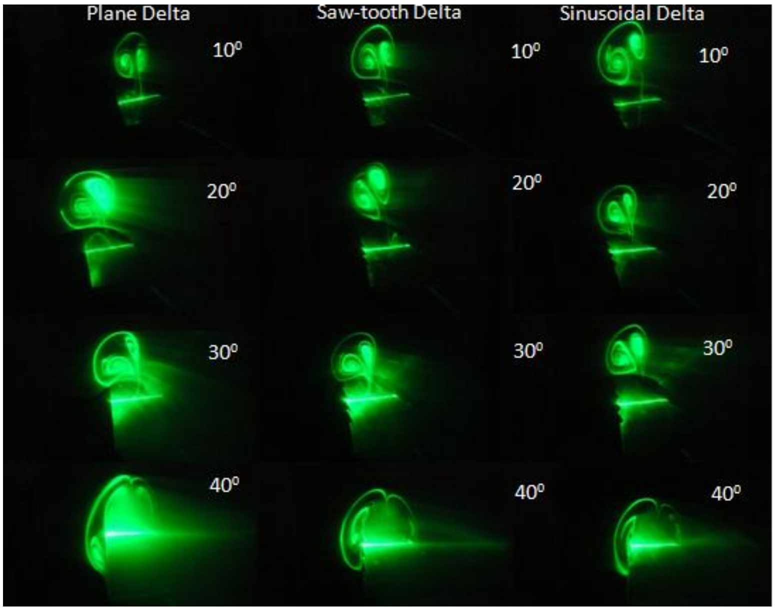

Figure 8. Laser-Smoke flow visualization of three different delta wings

4.2. Oil flow visualization

The oil flow mixture is sprayed on the surface of the delta wing. The mixture should be sprayed as very fine particles. Once the spraying of oil mixture is complete the model is kept inside the test section. The flow passing the delta wing model creates vortices on the surface of the wing, the size and shape of which is known by the alignment of the oil mixture according to the vortex patterns. The secondary attachment and secondary separation line are clearly seen with oil flow technique as demonstrated in figure 9.

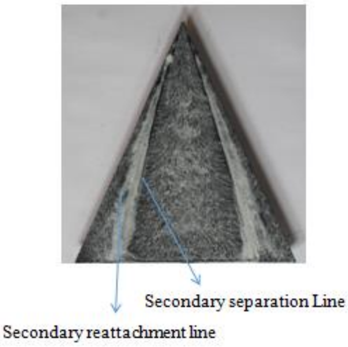

Figure 9. Oil flow visualization of plane delta at α = 20^0 and Re = $2.5x10^5$

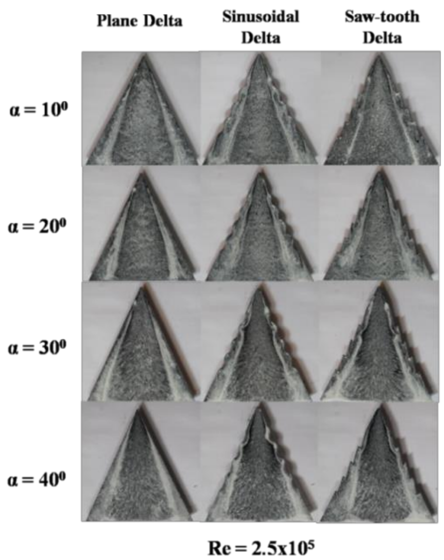

(a)

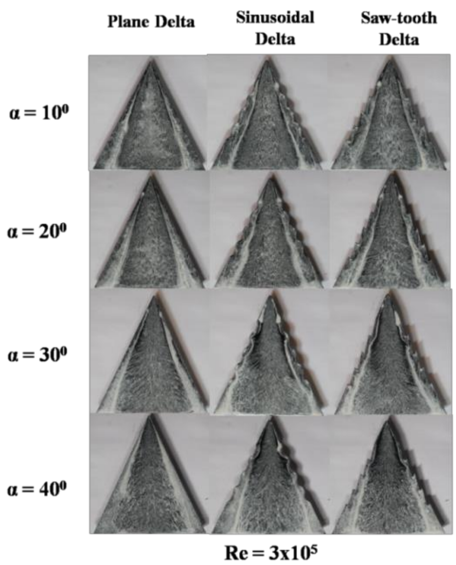

(b)

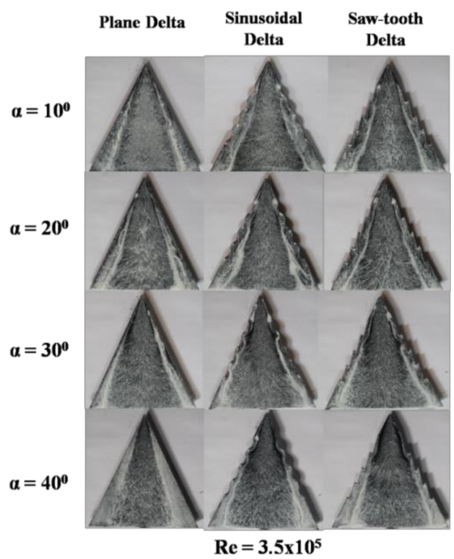

(c)

Figure 10. Oil flow visualization (a) Re = 2.5x10^5 (b) Re = 3x10^5 (c) Re = 3.5x10^5

Figure 10 (a) shows oil flow visualization performed on three delta wings at Re = 2.5×10^5 shows almost symmetric lines on two sides of delta wings for α = 10^0 & 20^0 with distinct separation and reattachment lines, which may be due to the formation of two symmetric vortices (primary and secondary vortices) on each side of the wings. At α = 30^0, delta wings shows curved and asymmetrical lines with a single thick line or slightly noticeable two lines on each side of the wings.

In this region, the thick line on each side of the wing appears to be formed by mixing of oil from separation line and reattachment lines, which may be due to flip flopping of vortices with moderate frequencies. At α = 40^0, plane delta shows perfect separation line only near to the apex, later this line spreads towards base indicating a vortex shedding with a turbulent wake formation. While sinusoidal and saw delta wings shows identifiable separation lines which are lengthier than the plane delta wing.

Figure 10 (b) shows clear separation and reattachment lines for plane delta wing at α = 10^o & 20^o. Plane delta wing shows almost straight lines while saw and sinusoidal wings shows curved lines for α = 10^0 & 20^0. At α = 30^0, all the three delta wings shows curved single thick separation line continuing till the end, which may be an indication of strong vortices compared to the previous case. At α = 40^0 plane delta after the apex shows wide region of random spreading of oil, which is an indication for fat and thick turbulent wake region. While for saw and sinusoidal delta wings, this region is confined near to the base and moreover they have shown thick separation lines after the apex, which may indicate that at α = 40^0, the vortices on saw and sinusoidal are stable than plane delta wing.

At α = 40^o, all the three delta wings, after the mid portion shows a thick lines which may be formed due to the forceful sweeping of oil caused by high rotational speeds. Such high velocity in vortices is possible only when the vortex is at certain distance above the surface. Hence, here it can be attributed to a situation of "vortex lift off" from the surface and trying to merge with the flow creating a low pressure region behind the body.

Figure 10 (c) shows thick and almost symmetric line pattern for the plane and sinusoidal delta wings. At α = 20^0 & 30^0 a single line found to be continuing till the base of the wings covering more than half of the root length, which may indicate increment in single vortex strength compared to previous two cases. At α = 40^0, plane delta shows increment in length of separation line compared to the previous two cases and also there is a decrement in random flow pattern area. It is understood from oil flow visualization that due to increment in Reynolds number, vortex strength increases for a given type of delta wing at a given angle of attack.

4.3. Computational results

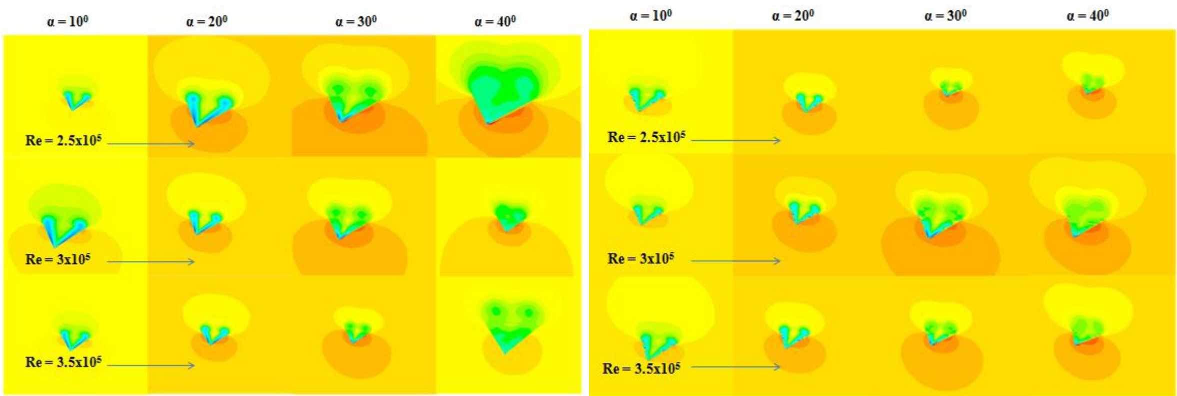

(a) **(b)**

IOP Conf. Series: Journal of Physics: Conf. Series **1276** (2019) 012008 doi:10.1088/1742-6596/1276/1/012008

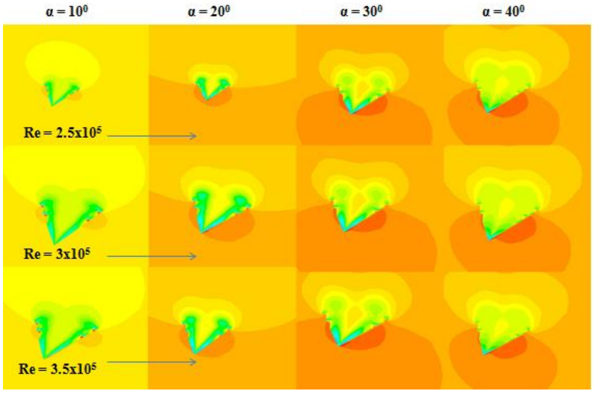

(c)

Figure 11. Pressure contours for (a) Plane delta (b) Sinusoidal delta (c) Saw tooth delta

Figures shows the static pressure contours on three delta wings at four angles of attack on mid plane where x/C = 0.5. Here thick blue colour indicates peak lowest pressure and red colour indicates highest pressure for a given case. Pressure contours reveal that the plane delta wing shows the strong low pressure contours for three Re at $\alpha = 10^o$ & 20^o, later the vortex strength completely diminishes at other higher angles. Saw toothed delta wings shows the attached low pressure region up to $\alpha = 40^o$ whereas plane and sinusoidal delta wings shows a completely turbulent flow at 40^0. The animation captured during the solution shows that vortices on three delta wings are symmetric and highly stable for $\alpha = 10^0$ & 20^0. Plane delta wing shows mild flip-flop of vortices at $\alpha = 20^0$. At $\alpha = 30^0$, the vortices starts shedding alternately with some frequency. This frequency of vortex shedding is very high in plane delta wing compared to other two configurations.

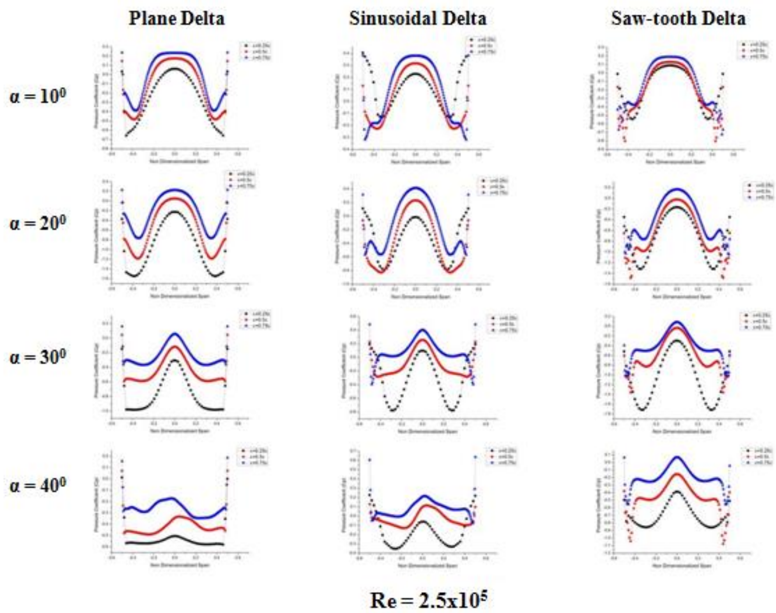

(a)

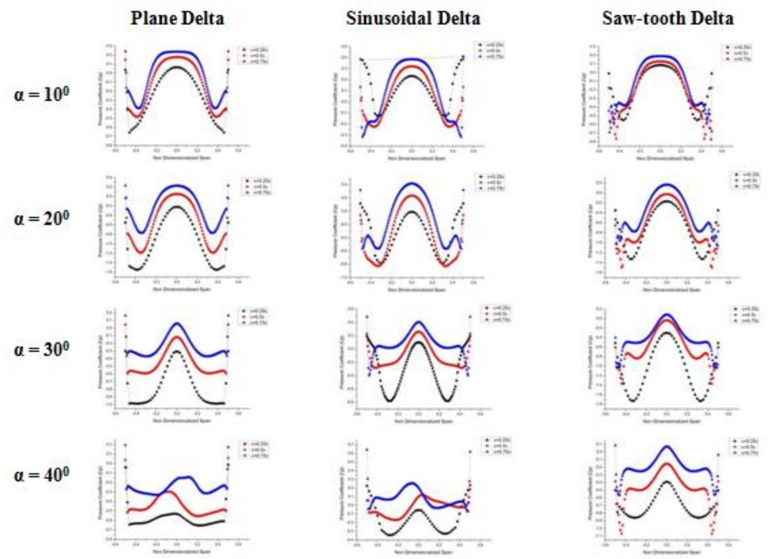

Re = 3x10^5

(b)

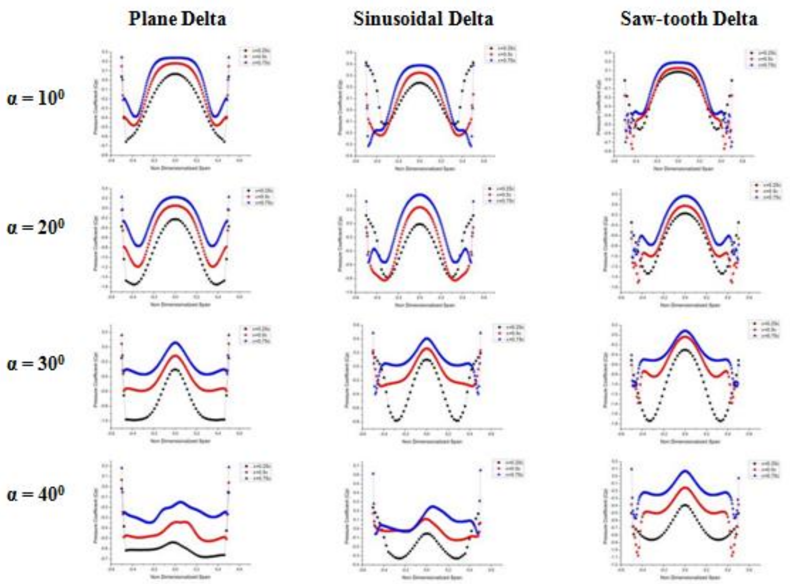

Re = 3.5x10^5

(c)

Figure 12. Plot of Cp at x/c = 0.25, 0.5, 0.75 for (a) Re = 2.5x10^5 (b) Re = 3x10^5 (c) Re = 3.5x10^5

Figure 11 (c) and 12 (a, b, c) says that the vortices in a saw-tooth delta wing is more stable at higher angles $\alpha = 40^o$ when compared to the sinusoidal and plane delta wing configuration. When we take a look at low angles we might come to know that plane delta is more efficient than other two configurations. The saw tooth and sinusoidal configurations shows a satisfactory behaviour at low α and good results at higher α. But plane delta wing shows better performance only at low α. When overall performance of the wing is in consideration, we come to a conclusion that saw tooth delta is more efficient when compared to the other two configurations.

4.4. Computational force coefficients

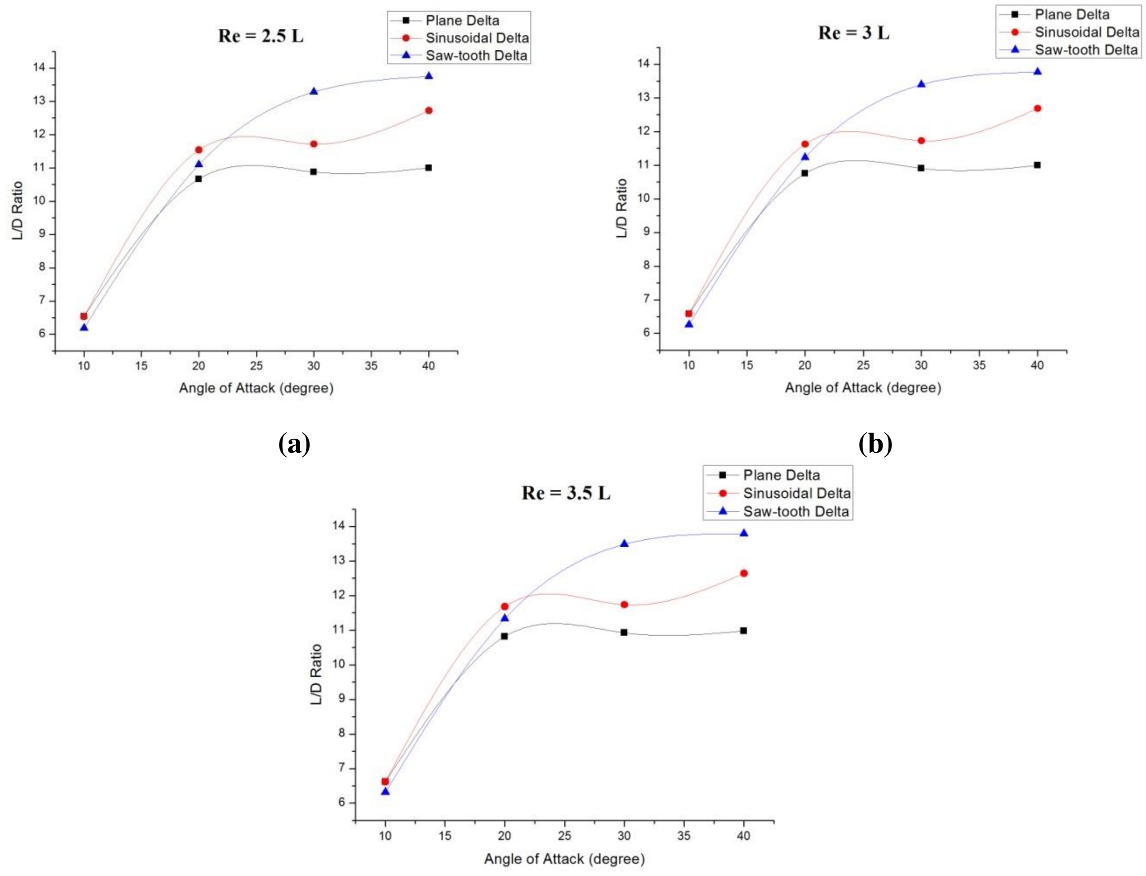

(c)

Figure 13. L/D ratio for all wings at (a) Re = 2.5x10^5 (b) Re = 3x10^5 (c) Re = 3.5x10^5

The value of C_L with respect to the angle of attack α, shows only a slight variation when compared with all wings at low angles of attack till α = 20^0. Plane delta wing gives better lift coefficient values at low angles of attack. But at high angles of attack, saw tooth delta shows better results at same flow conditions when compared to other wings. In order to get a better understanding of the results, we have plotted the L/D with respect to the angle of attack. We are able to see that the L/D ratio keeps increasing for saw tooth till α = 40^0.Therefore saw tooth delta wing is proven to be a better choice followed by sinusoidal delta wing as said by the values obtained by the L/D ratio which is considered to be one of the important aerodynamic parameters for an aircraft. At α = 30^0, both plane delta and sinusoidal delta wing shows a decrease in its L/D ratio whereas for the saw-tooth delta wing the ratio seems to be steadily increasing till 40^0.

5. Conclusions

From the experiments that were performed we have arrived at some conclusions as follows. Pressure contours at the mid plane suggests that vortices are more stable for a saw tooth delta wing even with increasing angles of attack which in turn prevents stall. The plot L/D ratio and α for all cases also suggests that saw-tooth delta has not stalled till α = 40^0 whereas the other two wings shows a slight decrease in L/D at α = 30^0.The lift coefficient of each wing does not vary much with increase in velocity. They nearly remain same for all Reynolds number. The lift coefficient for all three wings are almost similar at $\alpha = 10^0$ and 20^0.The L/D curve of each delta wing follows the same pattern for all three Reynolds number. When overall performance of the wing is monitored at all flow conditions, it is the saw-tooth profile leading edge that is comparably more efficient whereas the sinusoidal delta wing also is convincingly better when compared with a plane delta wing.

6. References

1. Sukanta Saha, Bireswar Majumdar. 'Experimental and Numerical study of Surface Flow Pattern on Delta Wing' International Journal of Emerging Technology and Advanced Engineering www.ijetae.com (ISSN 2250-2459, Volume 2, Issue 3, March 2012).
2. Huang Chen, Jin-Jun Wang. 'Vortex Structures for flow over a delta wing with sinusoidal leading edge'. Experimental Fluids (2014) 55:1761 DOI 10.1007/s00348-014-1761-1.
3. Hiromitsu KAWAZOE, Yuki NISHIMURA, Takashi MATSUNO, Gouji YAMADA, Kazuo YANAGIMOTO. 'Study of effect of Petit deltas at the leading edge of a main delta wing on the wing characteristics' Journal of Fluid Science and Technology.
4. C.Breitsamter. 'Unsteady flow phenomena associated with leading edge vortices'. Progress in Aerospace Science 44 (2008) 48-65.
5. Anthony M. Mitchell, Jean Delery. 'Research into vortex breakdown control'. Progress in Aerospace Science 37 (2001) 385-418.
6. Heuy-Dong Kim, Young-Ki Lee, Myoung-Hwan Sohn. 'A Study of the vertical flow over a delta wing with a leading edge extension'. Journal of thermal science Vol.2, No.4.
7. Russell M. Cummings, James R. Forsythe, Scott A. Morton, Kyle D. Squires. 'Computational Challenges in high angle of attack flow prediction'. Progress in Aerospace Sciences 39 (2003) 369-384.